Supporting Information

Lezmy et al. 10.1073/pnas.1708700114

SI Experimental Procedures

Primary Cultures of Hippocampal Neurons. Hippocampi were dissected out from neonate BALB/c mice brains (0–2 d old). Hippocampi were washed three times in a HBSS-based solution containing 4 mM $NaHCO_3$, 5 mM Hepes, and HBSS (Sigma), pH adjusted to 7.3–7.4 at 4 °C. Tissues were digested in a solution including 137 mM NaCl, 5 mM KCl, 7 mM Na_2HPO_4, 25 mM Hepes, 4.45 mg/mL trypsin type XI (Sigma), and 1,614 U/mL DNase type IV (Sigma), pH adjusted to 7.2 °C at 4 °C. Hippocampal tissues were incubated for 15 min in 37 °C and were washed again once with 5 mL HBSS/20% FBS and once with HBSS. The cells were dissociated in a HBSS solution including 13.15 mM $MgSO_4$ and 1,772 U/mL DNase type IV (Sigma). Next, the cells were mechanically triturated with fire-polished Pasteur pipettes. HBSS/20% FBS was added to the dissociated cells, and the mixture was centrifuged at 1,000 × *g* at 4 °C for 10 min. The supernatant was discarded, and a plating medium including MEM (Gibco), 24.7 mM glucose, 0.089 mg/mL transferrin (Calbiochem), GlutaMAX (Sigma), 0.75 U/mL insulin (Sigma), 10% FBS (Biological Industries), and B-27 (Gibco) was added to the pellet. The cells were resuspended in the plating medium with a fire-polished Pasteur pipette, and drops were added to glass coverslips coated with Matrigel in a 24-well plate. After 1 h of incubation at 37 °C, the plating medium was added to the wells. The day after plating and twice a week thereafter half of the medium was removed from the wells and was replaced with the same volume of a feeding medium (MEM, 26.92 mM glucose, 0.097 mg/mL transferrin, GlutaMAX, B-27, and 3 μM Ara-C; Sigma).

Acute Brain Slices. Three-week-old BALB/c mice were anesthetized and decapitated using procedures approved by the Institutional Animal Care and Use Committee of Tel Aviv University, and the brains were removed. Transversal slices (400 μM) were cut with a Vibratome (VT1200; Leica) in an oxygenated solution at 4 °C containing 1.25 mM NaH_2PO_4, 2.5 mM KCl, 7 mM $MgCl_2$, 25 mM $NaHCO_3$, 25 mM glucose, 87 mM NaCl, 75 mM sucrose, and 0.5 mM $CaCl_2$. The slices were transferred to an oxygenated artificial cerebrospinal fluid (ACSF) solution at 37 °C for 45 min and then were kept at room temperature.

Sodium Imaging. Sodium imaging was performed as described previously (40, 41) with several changes. The experiments were performed on cultured hippocampal neurons (14–16 DIV). Changes in fluorescence were acquired using an 80 × 80 pixel CCD camera (NeuroCCD-SMQ; RedShirtImaging) controlled with NeuroPlex software (RedShirtImaging). To distinguish the axon from other fine processes emerging from the soma, trains of five APs were elicited by delivering brief current steps via the somatic whole-cell pipette, and the SBFI fluorescence was acquired at a rate of 125 frames/s. The only process exhibiting a high-amplitude, rapidly rising and decaying sodium transient was identified as the axon. To detect the boundaries of the sodium flux in the AIS precisely, single APs were evoked repeatedly while images were acquired at a rate of 500 frames/s, and 50–100 trials were averaged.

Electrophysiology. Patch-clamp recording was performed in the whole-cell configuration. Signals were filtered at 2 kHz and digitized at 5 kHz. Signals were amplified using different amplifiers (Molecular Devices): Axopatch 200B for whole-cell patch recording of cultured hippocampal neurons and for axonal loose-patch recording, Axopatch 700B for hippocampal slices recording, and Axoclamp 2B for sodium-imaging experiments. For recording of primary cultures, the extracellular solution contained 160 mM NaCl, 2.5 mM KCl, 10 mM Hepes, 10 mM glucose, 1.2 mM Mg^{2+}, and 1.8 mM Ca^{2} (pH was adjusted to 7.3 with NaOH). For the experiments inspecting the intrinsic properties of hippocampal neurons and the sodium-imaging experiments, synaptic blockers were added to the extracellular solution: 30 μM picrotoxin, 10 μM bicuculline, 10 μM NBQX, and 10 μM AP5. For M-current recordings, 5 mM 4-AP, 20 μM ZD7288, and 1 μM TTX were added to the extracellular solution. Cells were held at −20 mV to open the M-currents and to inactivate residual voltage-dependent currents. A step to −40 mV was evoked for 1.5 s to deactivate the M-currents. Holding at −80 mV for 1 s before each protocol was used to measure the leak currents, which were subtracted later. In the experiments of chronic XE991 exposure involving recordings at different time points (1–48 h), untreated cells were also recorded to survey any possible variability, but no particular variance was observed in control untreated cells within the recording time window (1–48 h). Microelectrodes with resistances of 5–8 MΩ were pulled from borosilicate glass capillaries (Harvard Apparatus) and filled with an intracellular solution. For current-clamp recordings, the intracellular solution contained 135 mM KCl, 1 mM KATP, 1 mM MgATP, 2 mM EGTA, 1.1 mM $CaCl_2$, 10 mM Hepes, and 5 mM glucose (pH adjusted to 7.25 with KOH). For M-current recording, the intracellular solution contained 130 mM K-gluconate, 6 mM KCl, 1.1 mM EGTA, 10 mM Hepes, 2 mM Na_2ATP, 1 mM $MgCl_2$, and 0.1 mM $CaCl_2$. For sodium imaging, the intracellular solution contained 130 mM K-gluconate, 6 mM KCl, 2 mM $MgCl_2$, 10 mM Hepes, 4 mM NaCl, and 2 mM SBFI. The liquid junction potential was calculated and subtracted from the recorded voltage (−5 mV for recordings of cultured hippocampal neurons and −17 mV for recordings of CA1 pyramidal neurons from slices).

Recordings from hippocampal slices were performed in ACSF (125 mM NaCl, 1.25 mM NaH_2PO_4, 26 mM $NaHCO_3$, 3 mM KCl, 10 mM glucose, 2 mM $MgCl_2$, and 2 mM $CaCl_2$). The intracellular solution for slice recording contained 145 mM K-gluconate, 2 mM $MgCl_2$, 0.5 mM EGTA, 2 mM ATP-Tris, 0.2 mM Na_2GTP, and 10 mM Hepes. CA1 pyramidal neurons from acute slices do not fire spontaneously; therefore, no synaptic blockers were added in the extracellular solution. For prolonged recordings, the access resistance was less than 30 MΩ and did not vary by more than 10% throughout the experiment. All the electrophysiological experiments were performed at room temperature.

For dual-patch recordings, the axon of each cell was first detected by sodium imaging as described above. Another microelectrode filled with extracellular solution with a resistance of 15–20 MΩ was positioned at different points along the axon in loose-patch configuration. At each point along the axon, 100 single APs were elicited by delivering brief current pulses via the somatic electrode, and axonal action currents were simultaneously recorded. The axonal pipettes were coated to within ∼100 μm of the tip with Parafilm (Pechiney Plastic Packaging) to minimize stray capacitance. Currents were low-pass–filtered at 100 kHz (−3 dB, four-pole Bessel filter) and digitized at 200 kHz. To identify the time-lag between the somatic and the axonal signals precisely, we used the maximum value of the derivative (dV_m/dt) of the somatic APs. The signals were adjusted by alignment of the timing of the dV_m/dt of the somatic AP. The somatic and axonal signals were then averaged, and the time difference between their peaks was measured.

Immunostaining. XE991 and/or other compounds were added to hippocampal neurons from primary culture for 1, 4, 24, or 48 h

prior to staining, meaning that the cells were at the same age when fixed for immunostaining (16 DIV). For staining of hippocampal cultures, neurons were fixed in 4% paraformaldehyde (PFA) for 10 min and were washed three times in PBS. Permeabilization of the membrane was performed by adding 0.1% Triton X-100 (Sigma) in a blocking solution (PBS with 0.1% BSA and 5% goat serum) for 4 min. After one washing with PBS, blocking solution was added to the coverslips for 10 min. The primary antibodies were added to the neurons for 1 h at room temperature. The coverslips were washed twice with PBS for 10 min and were incubated with the secondary antibodies for 1 h at room temperature. After two washings with PBS, the coverslips were mounted in Gel Mount (Sigma). For acute immunohistochemistry, the slices were fixed by immersion in a solution containing 4% PFA, 4% sucrose, and 10× PBS (pH adjusted to 7.4) for 30 min and were washed three times in PBS. The slices were then permeabilized with 0.2% Triton X-100 (Sigma) in a blocking solution (0.1% BSA, 5% goat serum, and PBS) for 1 h. After three washes with PBS, the primary antibodies were added overnight at 4 °C. After three PBS washes, the secondary antibodies were added for 2 h. The slices were mounted in Gel Mount (Sigma) after three PBS washes. The primary antibodies used for immunostaining were rabbit α-K_v7.3 (1:150) (Alomone), mouse α-ankyrin G (1:500) (NeuroMab), mouse α-pan Na_v (1:100) (Sigma), mouse α-FGF14 (1:500) (NeuroMab), rabbit α-MAP2 (1:1,000) (Millipore), and purified guinea pig α-NeuN (1:1,000) (Millipore). The secondary antibodies used were donkey α-rabbit Cy3 (1:500) (Jackson), goat α-mouse Alexa488 (1:1,000) (Invitrogen), and goat α-guinea pig Alexa 633 (1:500) (Invitrogen).

Data Analysis and Statistics. For all experiments, data were usually collected from at least three different batches. Control cells were always collected from each batch to minimize possible variations between batches. All graphs were built with Prism 5 (GraphPad). Statistical tests were performed with Prism 5 and SPSS (IBM). In acute treatments (XE991 or carbachol) that were carried out in the same neuron, statistical comparisons between untreated and treated cells were performed with a two-tailed paired *t* test. In chronic treatments that were carried out in two independent groups of cells, statistical comparisons were performed with a two-tailed unpaired *t* test. When treatments involved more than two independent groups of cells, statistical comparisons were performed with one-way ANOVA and post hoc Tukey's multiple comparison test or one-way ANOVA and post hoc Fisher's least significant difference test. For treatments measuring the rate of evoked spike discharge, statistical comparisons were performed with repeated-measures ANOVA and a post hoc Bonferroni comparison test. Analyses of electrophysiological recordings were performed with pClamp 10.4 (Molecular Devices). Images from immunostaining experiments were obtained using confocal microscopy (Leica TCS SP5) with oil-immersion objectives of 63× for cultures or 40× for slices. Fields containing hippocampal neurons from primary cultures or CA1 pyramidal neurons from acute slices were indiscriminately selected. Images obtained from slices were acquired by merging z-stacks with a step size of 1 μm. AIS measurements were obtained with ImageJ (NIH). For cultured hippocampal neurons, the contours of the soma were determined by capturing the cells with brightfield microscopy and immunostaining of K_v7.3, Na_v, FGF14, and MAP2. Then, the soma–axon boundaries were determined by superimposing the brightfield and the immunofluorescence images. In hippocampal slices, labeling of NeuN and immunostaining of K_v7.3 and Na_v were used to localize the soma–axon boundaries.

Fluorescence-staining intensities of K_v7.3, Na_v, FGF14, and ankyrin G in the AIS were adjusted to be strong without reaching saturation. A line profile was drawn starting at the soma and extending down the axon, through and past the AIS. Staining intensity along the axon was plotted starting from the edge of the soma. The starting and endpoints of the AIS were set as half of the maximal intensity along the intensity plot. It was verified that half of the maximal intensity closely reflected the starting and ending boundaries picked by eye. The distances between the edge of the soma and these points were measured, and their subtraction was equal to the length of the AIS. For slices, image stacks were merged as a single image, and similar measurements were performed. For each experiment, the images were split into two groups, and the measurements were performed in blind independently by two different individuals. The results were compared before the data were pooled together. For the AIS: soma intensity ratio, the areas of the soma and of the K_v7.3 or Na_v AIS segment were selected. The mean intensity was measured for the soma and AIS areas, and then the ratio between AIS and soma intensities was calculated. In addition, a K_v7.3: AnK G fluorescence intensity ratio in the AIS was calculated by selecting the K_v7.3 and AnK G segments in the same cell.

For the measurements of sodium flux boundaries in the SBFI sodium-imaging experiments, the edges of the soma were determined as the decay of the intensity to about half of the maximum intensity in the soma (40). The start and the end of the Na^+ influx were selected as the points where the fast Na^+ transients first appeared and disappeared completely, respectively. Each pixel along the axon was selected, and the traces were imported from NeuroPlex to Clampfit of pClamp 10.4 to calculate the amplitude of the sodium flux for each group of pixels. The images of the cells were imported from NeuroPlex to ImageJ to convert the start and end values from pixels to distances in micrometers (the dimensions of one pixel were 1 × 1 μm). The dispersion of the sodium flux was calculated by subtracting the starting point from the end of the Na^+ flux.

Modeling. Numerical simulations were performed in the NEURON 7.4 simulation environment (47) using a simplified compartmental model that encompassed the fundamental morphological and electrical features of CA1 pyramidal neurons. In the model, the diameter of the AIS section was constant (1.2 μm). The AIS was divided into two subsegments: the passive one (length, 5–20 μm) and the one containing Na_v and K_v7 channels (35 μm). In most models, the initial length of the passive subsegment was 10 μm. The subsequent axonal segment (length, 200 μm; diameter, 1.2 μm) was myelinated. The soma (length, 35 μm; diameter, 23 μm) gave rise to a single apical dendrite (length, 700 μm; diameter, 3.5 μm) and to two basal dendrites (length, 200 μm; diameter, 1.2 μm). For computational precision, all compartments were divided into many segments, with the length of individual segments usually less than 1 μm. Unless otherwise stated, the passive electrical properties R_m, C_m, and R_i were set to 15,000 Ω/cm^2, 0.9 μF/cm^2, and 125 Ω/cm, respectively, uniformly throughout all compartments. Myelination was simulated by reducing Cm to 0.02 μF/cm^2. The resting membrane potential at the soma was set to −68 mV. All simulations were run with 5-μs time steps, and the nominal temperature of simulations was 22 °C. The model incorporated a Hodgkin–Huxley–based Na^+ conductance as previously described (41) and M-channel–based conductance (27). Unless otherwise stated, the Na^+ conductance was 2,000 pS/μm^2, and the M-channel conductance varied from 0 to 666 pS/μm^2 in the active subsegment of the AIS. The active subsegment also included a high-voltage–activated K_v channel and a faster low-voltage–activated K_v1-like potassium channel distributed as described in ref. 48. Namely, the density of K_v and K_v1 was set to 20 and 100 pS/μm^2, respectively, at the proximal edge of the subsegment, and it increased linearly with the distance toward the distal edge to 2,000 pS/μm^2.

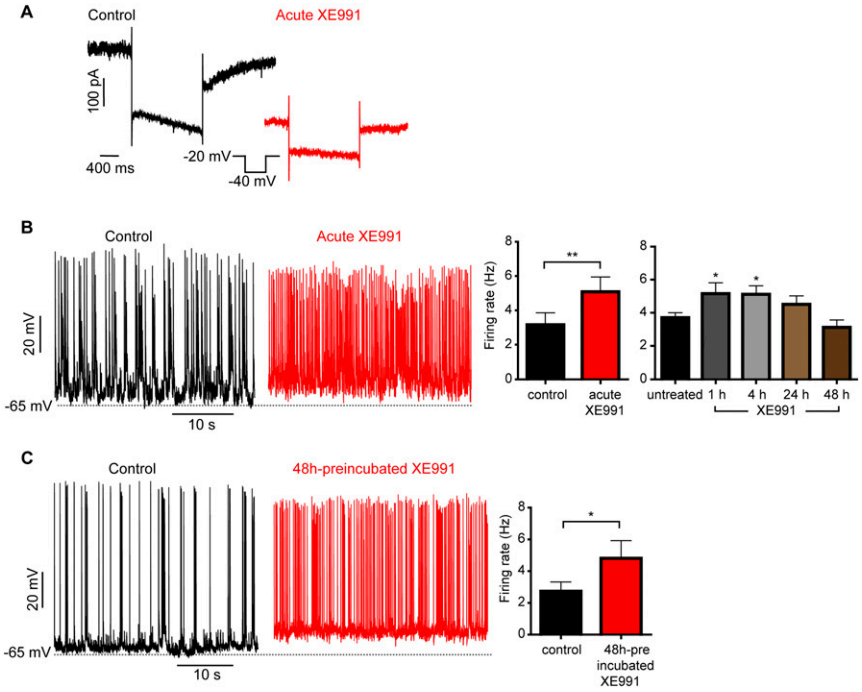

Fig. S1. XE991 inhibits the M-current and affects the spontaneous firing rate in cultured hippocampal neurons. (*A*) Representative M-currents, measured by the standard deactivation protocol (holding at −20 mV and deactivation at −40 mV), were inhibited following acute exposure to 10 μM XE991. (*B*, *Left*) Representative traces showing the larger spontaneous firing rate after acute XE991 treatment. (*Center*) Acute XE991 exposure significantly increased the spontaneous firing rate by 1.7-fold (two-tailed paired *t* test: $^{**}P = 0.0012$, $n = 11$, $t = 4.495$, df = 10). (*Right*) With longer exposures to XE991, the spontaneous firing rate progressively decreased and returned to close to the values of untreated neurons [one-way ANOVA: $^{*}P = 0.0145$, F = 3.186, df = 4; and post hoc Tukey's multiple comparison test: significantly different for untreated ($n = 84$) vs. 1 h ($n = 21$), untreated vs. 4 h ($n = 39$), untreated vs. 24 h ($n = 37$), and untreated vs. 48 h ($n = 26$)]. (*C*, *Left*) Representative traces of spontaneous firing when XE991 was preincubated in the feeding medium for 48 h at 37 °C and was then exposed acutely to hippocampal neurons. (*Right*) Under these conditions, XE991 significantly increased the spontaneous firing rate, showing that XE991 is not degraded during the chronic exposure (two-tailed paired *t* test: $^{*}P = 0.0130$, $n = 9$, $t = 3.177$, df = 8).

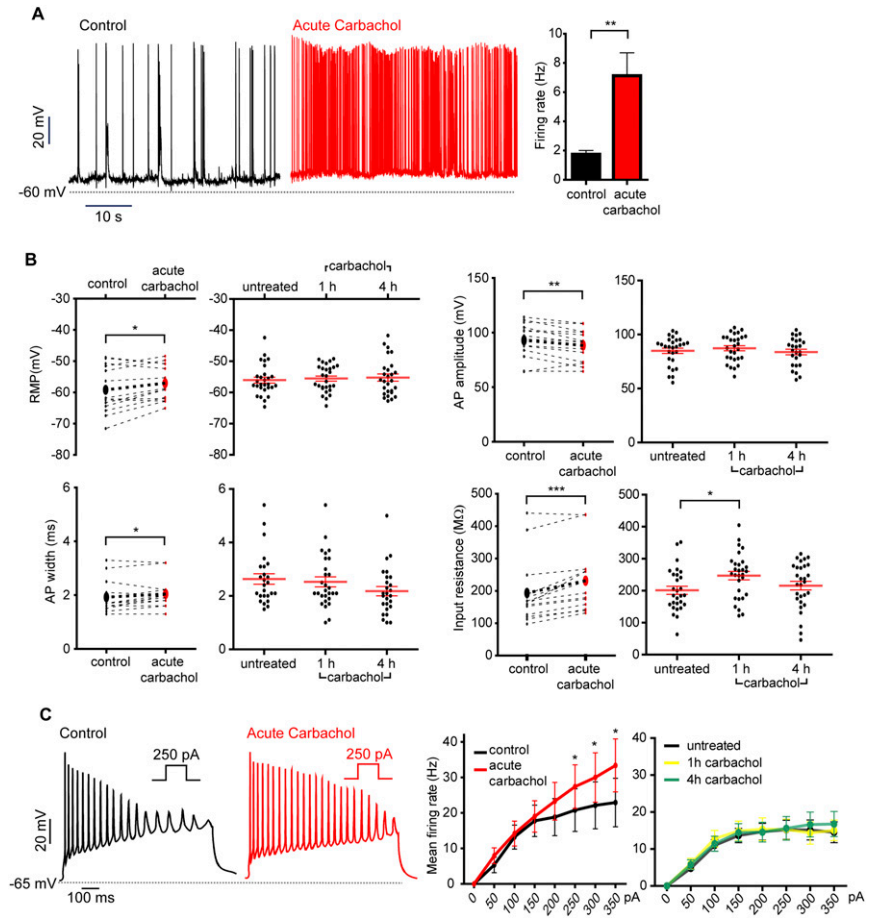

Fig. S2. Effect of carbachol treatment on the excitability of cultured hippocampal neurons. (*A*, *Left*) Representative traces showing the larger spontaneous firing rate following acute carbachol treatment (10 μM). (*Right*) Acute carbachol exposure significantly increased the spontaneous firing rate by 4.1-fold (two-tailed paired *t* test: $^{**}P = 0.0035$, $n = 14$, $t = 3.552$ df = 13). (*B*, *Upper Left*) Acute carbachol treatment depolarized the RMP (two-tailed paired *t* test: $^{*}P = 0.0151$, $n = 14$, $t = 2.797$, df = 13), which upon extended exposure progressively repolarized and returned to close to the values of untreated neurons [one-way ANOVA: $P = 0.8336$, F = 0.1825, df = 2, and post hoc Tukey's multiple comparison test: not significantly different for untreated ($n = 28$) vs. 1 h ($n = 28$) and untreated vs. 4 h ($n = 27$)]. (*Upper Right*) Acute carbachol treatment decreased the AP amplitude (two-tailed paired *t* test: $^{**}P = 0.0058$, $n = 14$, $t = 3.292$, df = 13), which upon extended exposure progressively returned to close to the values of untreated neurons [one-way ANOVA: $P = 0.5966$, F = 0.5200, df = 2, and post hoc Tukey's multiple comparison test: not significantly different for untreated ($n = 28$) vs. 1 h ($n = 28$) and untreated vs. 4 h ($n = 25$)]. (*Lower Left*) Acute carbachol exposure significantly increased the AP width (two-tailed paired *t* test: $^{*}P = 0.0447$, $n = 14$, $t = 2.222$, df = 13), which following prolonged exposure progressively decreased [one-way ANOVA: $P = 0.2069$, F = 1.609, df = 2, and post hoc Tukey's multiple comparison test: not significantly different for untreated ($n = 25$) vs. 1 h ($n = 28$) and untreated vs. 4 h ($n = 26$)]. (*Lower Right*) Acute carbachol exposure significantly increased the input resistance (two-tailed paired *t* test: $^{***}P = 0.0002$, $n = 14$, $t = 5.261$ df = 13), which following 4-h exposure returned to close to the values of untreated neurons [one-way ANOVA: $^{*}P = 0.0493$, F = 3.121, df = 2, and post hoc Tukey's multiple comparison test: significantly different for untreated ($n = 28$) vs. 1 h ($n = 29$) and not significant for untreated vs. 4 h ($n = 29$)]. (*C*, *Left*) Representative spike discharge evoked by 800-ms steps injection of depolarizing current with increments of 50 pA in the presence or absence of 10 μM carbachol. (*Center*) Acute XE991 treatment significantly increases the rate of evoked spike discharge ($n = 14$; two-tailed paired *t* test: 50 pA, $P = 0.3144$, $t = 1.047$, df = 13; 100 pA: $P = 0.3314$, $t = 1.009$, df = 13; 150 pA: $P = 0.4722$, $t = 0.7404$, df = 13; 200 pA: $P = 0.0862$, $t = 1.857$, df = 13; 250 pA: $^{*}P = 0.0469$, $t = 2.196$, df = 13; 300 pA: $^{*}P = 0.049$, $t = 2.172$, df = 13; 350 pA: $^{*}P = 0.0136$, $t = 2.853$, df = 13). (*Right*) In chronic carbachol treatment, the rates of spike discharge were not significantly different from untreated neurons (control: $n = 24$; 1 h: $n = 21$; 4 h: $n = 23$). Repeated-measures ANOVA: $P = 0.95$, F = 0.051, df = 2.

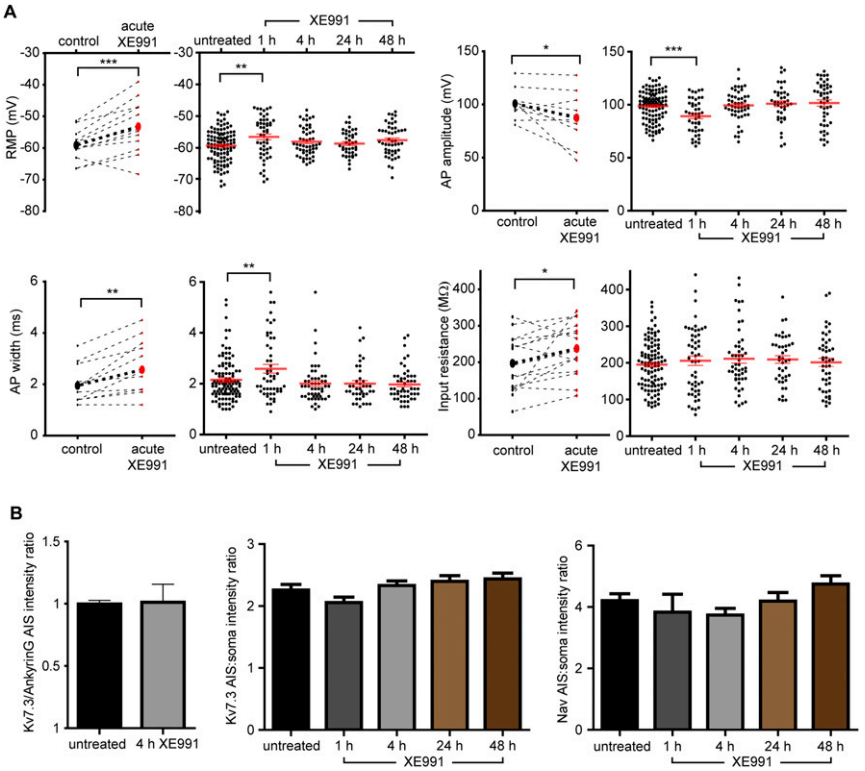

Fig. S3. Effect of XE991 treatment on excitability and on $K_v7.3$ and Na_v immunofluorescence intensities in cultured hippocampal neurons. (*A*, *Upper Left*) Acute XE991 treatment depolarized the RMP (two-tailed paired *t* test: ***$P = 0.0007$, $n = 13$, $t = 4.552$ df = 12), which upon extended exposure progressively repolarized and returned close to the values of untreated neurons [one-way ANOVA: $P = 0.0221$, F = 2.903, df = 4, and post hoc Tukey's multiple comparison test: significantly different, **$P = 0.0096$ for untreated ($n = 109$) vs. 1 h ($n = 51$) and not significantly different for untreated vs. 4 h ($n = 52$), untreated vs. 24 h ($n = 42$), and untreated vs. 48 h ($n = 49$)]. (*Upper Right*) Acute XE991 treatment decreased the AP amplitude (two-tailed paired *t* test: *$P = 0.0454$, $n = 10$, $t = 2.321$ df = 9), which after extended exposure progressively returned to close to the values of untreated neurons [one-way ANOVA: $P = 0.0014$, F = 4.565, df = 4, and post hoc Tukey's multiple comparison test: significantly different, ***$P = 0.0005$ for untreated ($n = 111$) vs. 1 h ($n = 44$) and not significantly different for untreated vs. 4 h ($n = 50$), untreated vs. 24 h ($n = 40$), and untreated vs. 48 h ($n = 48$)]. (*Lower Left*) Acute XE991 exposure significantly increased the AP width (two-tailed paired *t* test: **$P = 0.0013$, $n = 13$, $t = 4.182$ df = 12), which after prolonged exposure progressively decreased [one-way ANOVA: **$P = 0.0015$, F = 4.509, df = 4, and post hoc Tukey's multiple comparison test: significantly different for untreated ($n = 108$) vs. 1 h ($n = 51$) and not significantly different for untreated vs. 4 h ($n = 52$), untreated vs. 24 h ($n = 39$), and untreated vs. 48 h ($n = 51$)]. (*Lower Right*) Acute XE991 exposure significantly increased the input resistance (two-tailed paired *t* test: *$P = 0.0314$, $n = 15$, $t = 2.391$, df = 14), which after extended exposure progressively returned to close to the values of untreated neurons [one-way ANOVA: $P = 0.7150$, F = 0.5284, df = 4, and post hoc Tukey's multiple comparison test: not significantly different for untreated ($n = 105$) vs. 1 h ($n = 52$), untreated vs. 4 h ($n = 49$), untreated vs. 24 h ($n = 41$), and untreated vs. 48 h ($n = 46$)]. (*B*, *Left*) The $K_v7.3$:ankyrin G intensity ratios were not significantly different before and after 4 h treatment with XE991 (two-tailed unpaired *t* test: $P = 0.9219$, $t = 0.09831$ df = 114; untreated, $n = 55$; XE991, $n = 61$). (*Center*) The $K_v7.3$ AIS:soma intensity ratios were not significantly different before and after treatment with XE991 [one-way ANOVA: $P = 0.0554$, F = 2.327, df = 4, and post hoc Tukey's multiple comparison test: not significantly different for untreated ($n = 123$) vs. 1 h ($n = 70$), untreated vs. 4 h ($n = 109$), untreated vs. 24 h ($n = 84$), and untreated vs. 48 h ($n = 89$)]. (*Right*) Na_v AIS:soma intensity ratios were not significantly different before and after treatment with XE991 [one-way ANOVA: $P = 0.1367$, F = 1.763, df = 4, and post hoc Tukey's multiple comparison test: not significantly different for untreated ($n = 68$) vs. 1 h ($n = 26$), untreated vs. 4 h ($n = 62$), untreated vs. 24 h ($n = 62$), and untreated vs. 48 h ($n = 46$)].

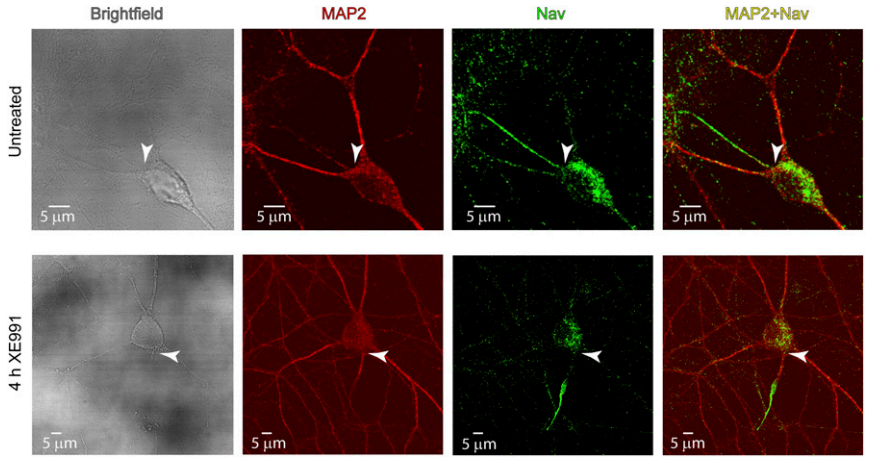

Fig. S4. M-channel inhibition triggers a distal shift of AIS Na_v channels. (*Upper Row*) Representative Na_v and MAP2 coimmunostaining of an untreated neuron. Shown are brightfield, MAP2-labeled, panNa_v-labeled, and merged images. (*Lower Row*) Representative Na_v and MAP2 coimmunostaining of a neuron exposed to 10 µM XE991 for 4 h. Shown are brightfield, MAP2-labeled, panNa_v-labeled, and merged images.

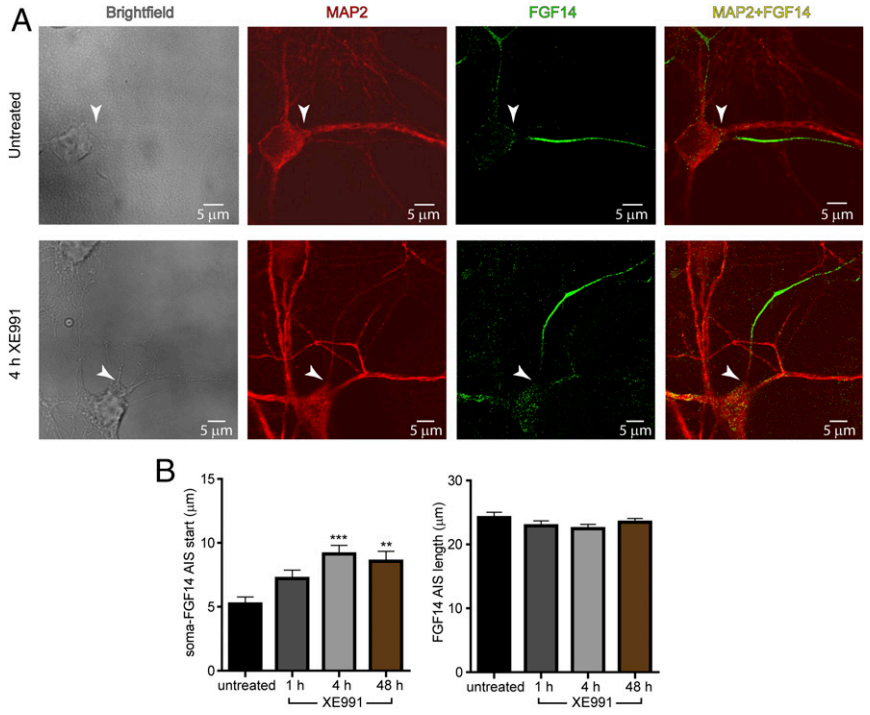

Fig. S5. M-channel inhibition triggers a fast distal shift of AIS FGF14. (*A*, *Upper Row*) Representative Na_v and MAP2 coimmunostaining of an untreated neuron. Shown are brightfield, MAP2-labeled, FGF14-labeled, and merged images. (*Lower Row*) Representative Na_v and MAP2 coimmunostaining of a neuron exposed to 10 µM XE991 for 4 h. Shown are brightfield, MAP2-labeled, FGF14-labeled, and merged images. (*B*, *Left*) The FGF14 segment is significantly shifted distally. The distances from the soma to the start of the FGF14 label following the indicated duration of XE991 exposure are significantly different from those in the untreated neuron: one-way ANOVA: ***$P = 0.0002$, $F = 6.573$ df = 3, and post hoc Tukey's multiple comparison test: significantly different for untreated ($n = 107$) vs. 4 h ($n = 120$) and **$P = 0.0056$ untreated ($n = 100$) vs. 48 h ($n = 121$); for 1 h ($n = 100$). (*Right*) The length of the FGF14 segment in the AIS does not change significantly throughout XE991 exposure (untreated, $n = 107$; 1 h, $n = 100$; 4 h, $n = 120$; and 48 h, $n = 121$: one-way ANOVA, $P = 0.3662$, $F = 1.059$ df = 3).

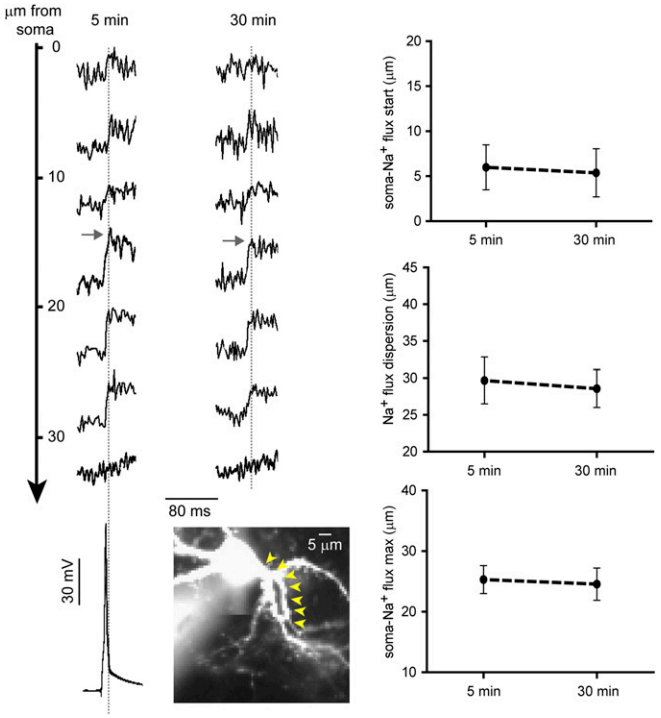

Fig. S6. The location and distribution of sodium flux changes in the AIS remain stable during prolonged recording under control conditions. (*Left*) Representative Na^+ flux changes were tracked on the same cell without any treatment for 30 min. Cells were patch-clamped and filled with SBFI. In the whole-cell configuration, a single AP was evoked, and Na^+ imaging was performed simultaneously. Areas of 5 μm along the axon were selected, and changes in Na^+ fluxes were tracked along these areas (yellow arrowheads). (*Right*) The distance from the start of sodium flux in the AIS to the soma (*Top*; two-tailed paired *t* test, $P = 0.2456$, $n = 3$, $t = 1.625$ df = 2), the dispersion of the sodium flux (*Middle*; two-tailed paired *t* test, $P = 0.2093$, $n = 3$, $t = 1.826$ df = 2), and the distance of the peak Na^+ flux changes to the soma (*Bottom;* two-tailed paired *t* test, $P = 0.1835$, $n = 3$, $t = 2.000$ df = 2) did not change significantly during prolonged recording under control conditions.

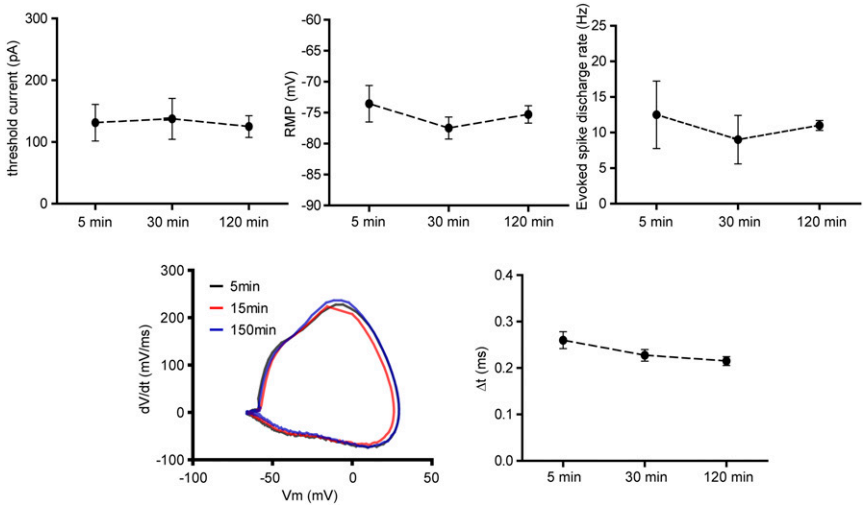

Fig. S7. The intrinsic excitability properties of CA1 pyramidal neurons from hippocampal slices remain stable during prolonged recording under control conditions. CA1 pyramidal neurons were whole-cell patch-clamped, and their activity was monitored for 2 h under control conditions. (*Upper*) The threshold current (two-tailed paired *t* test: $P = 0.3910$, $n = 4$, $t = 1.000$, df = 3), the RMP (two-tailed paired *t* test: $P = 0.06$, $n = 4$, $t = 3.186$, df = 3), and the evoked spike discharge rate (two-tailed paired *t* test: $P = 0.1402$, $n = 4$, $t = 1.993$, df = 3) did not change significantly during prolonged recording under control conditions. (*Lower Left*) Single-AP phase plots of the first derivative (dV_m/dt) against voltage from the same cell at 5 min, 15 min, and 150 min were very similar during prolonged recording. (*Lower Right*) The lag time between the AIS and the somatic phases derived from the second derivative (dV_m/dt^2) of single APs at 5 min, 30 min, and 120 min were similar during prolonged recording (two-way ANOVA and post hoc Bonferroni comparison tests: $P = 0.1581$, F = 2.55, DFn = 2, DFd = 6, $n = 4$).

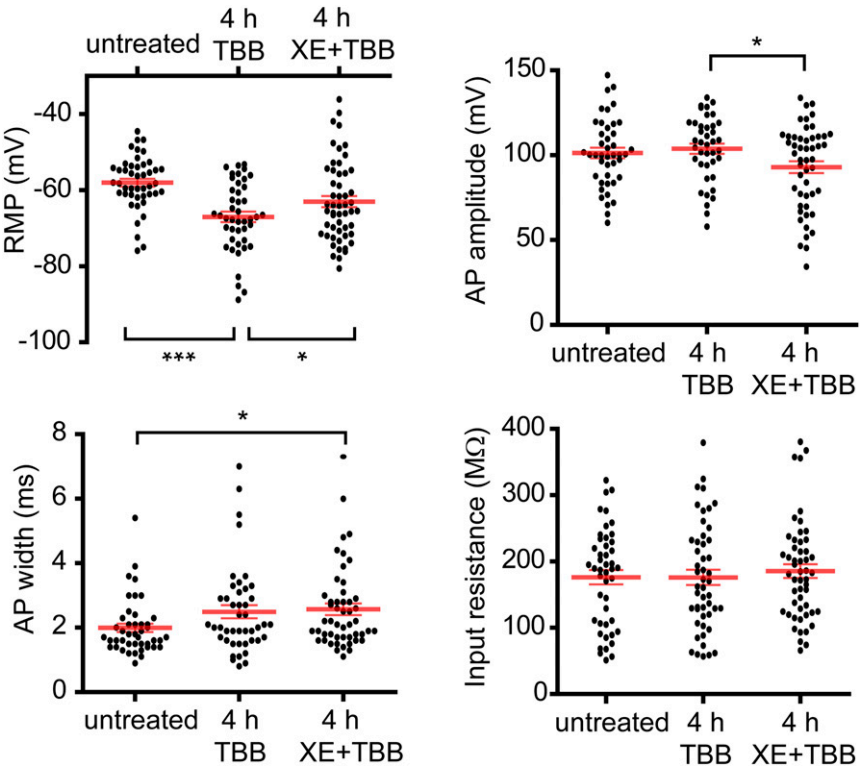

Fig. S8. The CK2 inhibitor TBB prevents the rapid adaptive changes in neuronal excitability following chronic XE991 exposure. (*Upper Left*) TBB alone caused a significant hyperpolarization of the RMP; however the RMP depolarized again following 4 h exposure to XE991+TBB compared with TBB alone [one-way ANOVA and post hoc Fisher's least significant difference test: ***$P < 0.0001$ for untreated ($n = 45$) vs. 4 h TBB ($n = 44$); **$P = 0.007$ for untreated vs. 4 h XE+TBB ($n = 53$); *$P = 0.032$ for 4 h TBB vs. 4 h XE+TBB]. (*Upper Right*) The AP amplitude decreased following chronic XE991 exposure together with TBB compared with the AP amplitude of TBB only [one-way ANOVA and post hoc Fisher's least significant difference: $P = 0.601$ (not significantly different) for untreated ($n = 43$) vs. 4 h TBB ($n = 40$), but *$P = 0.02$ (significantly different) for 4 h TBB vs. 4 h XE+TBB ($n = 50$)]. (*Lower Left*) The AP width of neurons exposed to XE991+TBB for 4 h increased compared with that of untreated neurons [one-way ANOVA and post hoc Fisher's least significant difference test: $P = 0.199$ (not significantly different) for untreated ($n = 44$) vs. 4 h TBB ($n = 44$), but *$P = 0.011$ (significantly different) for untreated vs. 4 h XE+TBB ($n = 50$)]. (*Lower Right*) The input resistance was not affected by 4 h TBB or 4 h XE+TBB [one-way ANOVA and post hoc Fisher's least significant difference: not significantly different in untreated ($n = 46$) vs. 4 h TBB ($n = 49$) ($P = 0.980$), in untreated vs. 4 h XE+TBB ($n = 52$) ($P = 0.560$), or in 4 h TBB vs. 4 h XE+TBB ($P = 0.536$)].

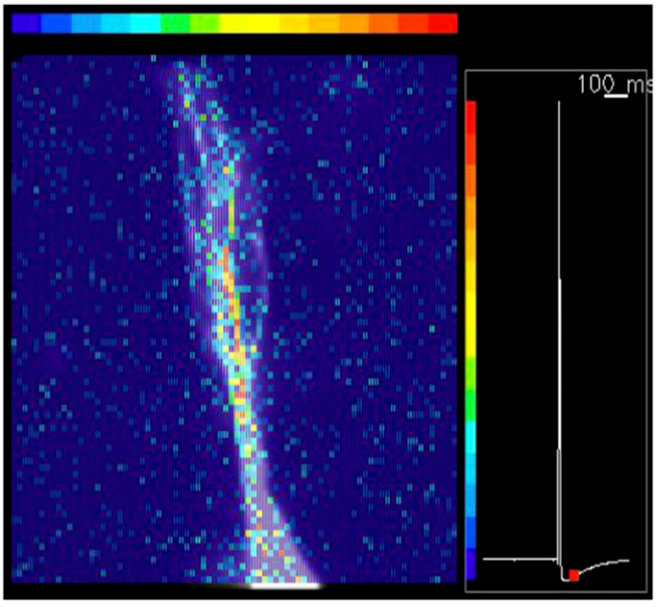

Movie S1. Sodium flux changes in the AIS of an untreated neuron. Na^+ flux changes in the axon were induced by single APs, and recordings were performed using SBFI as described in Fig. 3.

Movie S1

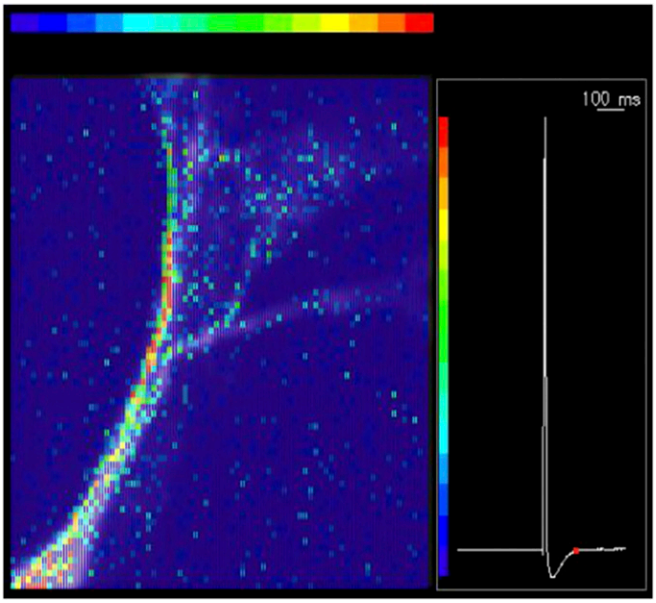

Movie S2. Sodium flux changes in the AIS of a neuron exposed to XE991 for 4 h. Na^+ flux changes in the axon were induced by single APs, and recordings were performed using SBFI as described in Fig. 3.

Movie S2